IEEE Access
Multidisciplinary | Rapid Review | Open Access Journal

Received 11 January 2024, accepted 10 April 2024, date of publication 3 May 2024, date of current version 10 May 2024.

*Digital Object Identifier 10.1109/ACCESS.2024.3396642*

RESEARCH ARTICLE

# Short Packet Communications for Relay Systems With Co-Channel Interference at Relay: Performance Analysis and Power Control

**QUANG-SANG NGUYEN[1], UYEN-VU LE ANH[1], TAN N. NGUYEN[2], (Member, IEEE), TIEN-TUNG NGUYEN[3], AND MIROSLAV VOZNAK[4], (Senior Member, IEEE)**

[1]Science and Technology Application for Sustainable Development Research Group, Ho Chi Minh City University of Transport, Ho Chi Minh City 700000, Vietnam
[2]Communication and Signal Processing Research Group, Faculty of Electrical and Electronics Engineering, Ton Duc Thang University, Ho Chi Minh City 70000, Vietnam
[3]Faculty of Electronics Technology, Industrial University of Ho Chi Minh City (IUH), Ho Chi Minh City 700000, Vietnam
[4]Faculty of Electrical Engineering and Computer Science, VSB—Technical University of Ostrava, 70800 Ostrava, Czech Republic

Corresponding author: Tan N. Nguyen (nguyennhattan@tdtu.edu.vn)

This work was supported in part by European Union within the REFRESH Project—Research Excellence for Region Sustainability and High-Tech Industries of European Just Transition Fund under Grant CZ.10.03.01/00/22_003/0000048; and in part by the Ministry of Education, Youth and Sports of the Czech Republic (MEYS CZ) through the Project SGS conducted by the VSB—Technical University of Ostrava under Grant SP 7/2023.

**ABSTRACT** In this paper, we evaluate short packet communication (SPC) for a cooperative system where one relay assists data transmission between one multi-antenna source and one single antenna destination with the presence of co-channel interference at the relay. Two transmission schemes, i.e., transmit antenna selection (TAS) scheme and beamforming scheme (BF), are considered. Based on metric of SPC, we derive the average block error rate (BLER) for the system in asymptotic and closed-form expressions for both schemes. In addition, a solution of optimal power allocation (OPA) to maximize end-to-end effective system throughput is proposed. Effects of parameters such as total transmit power, number of the source's antennas, number of co-channel interference, and packet length on the performance of the system are evaluated. Finally, the results reveal that the performance of the OPA scheme outperforms that of the benchmark scheme, i.e., equal power allocation solution, in terms of BLER and the effective throughput for both the TAS and BF schemes. Moreover, the performance of the system reaches to saturation value with more antennas at the source. The findings indicate that the TAS and BF schemes have the same performance in terms of both the BLER and the effective throughput.

**INDEX TERMS** Block error rate, cooperative system, co-channel interference, short packet communications.

## I. INTRODUCTION

Recently, short packet communication (SPC) has been considered as an important technique for achieving low latency in wireless communication systems, and it has been widely studied in literature. Several scenarios such as cognitive radio networks [1], device-to-device (D2D) networks [2], unmanned-aerial-vehicle (UAV) networks [3], [4], relaying systems [5], [6], [7] have been investigated in SPC systems.

Furthermore, many applications where the transmitter and destination nodes cannot communicate directly with each other. Relaying communication is a technique in wireless communication where an intermediate device is used to forward data packets between the transmitter and the receiver [8], [9]. The relaying device, also known as a relay node or relay station, receives the information from

The associate editor coordinating the review of this manuscript and approving it for publication was Wei Feng.

the transmitter and re-transmits it to the receiver. Two well-known protocols such as decode-and-forward (DF), and amplify-and-forward (AF) [10], [11] have been used in cooperative networks. An evaluation of the AF relay system performance with taking into account interference at the relay was discussed in [12]. Inspired by [12], outage performance of an AF system under Nakagami-$m$ channel evaluated in [13].

Integrating SPC into cooperative systems is to take advantage of low latency and extended coverage. Due to this reason, the integration has been investigated in several wireless applications. In [14] the end-to-end (e2e) block error rate (BLER) for a multiple-input multiple-output system was derived, and a solution to determine the minimal value of the e2e BLER was proposed. Considering goodput, and energy efficiency of a full-duplex system, the authors evaluated the system based on calculating the BLER and outage probability [5]. In [6], via BLER, the authors compared the performance of two schemes, i.e., direct transmission and incremental relaying schemes. Considering successive interference cancellation imperfection, the average BLERs were derived in a system where one unmanned aerial vehicle acts as a relay [7]. Deploying both AF and DF, the performance system in terms of BLER of a cooperative network where a relay is shared for cellular network and Internet of Things (IoT) network was evaluated [15]. The authors of [16] used machine learning as a novel tool for addressing the throughput maximization of a multi-hop network with SPC. With the effective combination of AF and DF protocols, the authors in [17] proposed a new relay protocol that achieves performance advantages and saves transmission power. The authors of [18] compared average BLER of a cooperative system under full-duplex mode between long-packet and short-packet communication. A solution to determine the minimum value of total transmit power by optimizing a combination of several factors, i.e. decoding error probability, relay selection, and transmit power allocation for multi-relay systems have been proposed in [19]. In order to improve performance of a non-orthogonal multiple access (NOMA)-based cooperative system, the authors in [20] proposed an adaptive hybrid relaying protocol by selecting appropriate transmission modes. However, these works only focused on investigating performance system without co-channel interference.

Different from [12] and [13], where the performance of the systems evaluated under infinite block length packet and power optimization was ignored [12], [13], we consider a relaying system with short packet communications. Unlike [21], where DF relay protocol was deployed while we adopt AF relay system. Despite exploiting AF relay, the system of [22] with single antenna at all terminals was disregarded co-channel interference, however, our system considers multiple antennas at the source and the interference at the relay.

The list of important contributions is shown as follows:

1) In contrast to [12], [13], [21] and [22], we investigate SPC for a relaying system consisting of one multiple antenna transmitter source, one AF relay under co-channel interference and one single antenna destination.
2) Due to multiple antenna at the source, we take into account two transmission schemes, namely transmit antenna selection (TAS) scheme and beamforming scheme using maximum ratio transmission (BF-MRT).
3) With this setting, we calculate the closed-form expressions of the average BLER of the system, then derive the asymptotic of the average BLER. In particular, we propose a solution to control the transmit powers of the system with the aim of maximizing effective throughput.
4) To verify the correctness of the analytical results, we conduct extensive numerical simulations. Moreover, the performance of the system is evaluated under the effects of the number of antennas at the transmitter source, packet lengths, and the number of interferers.

For clarity, we show differences between this paper with the related works in Table 1.

*Organization:* We introduce the system model in Section II. Next, Section III and Section IV provide an analysis of the performance system and propose a solution for maximizing end-to-end effective throughput, respectively. Finally, Section V and Section VI describe the numerical results and the conclusions, respectively.

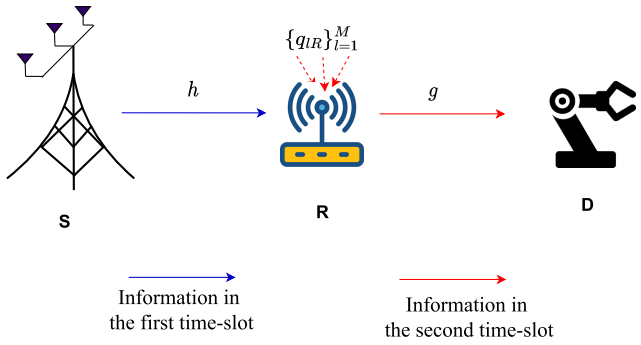


**FIGURE 1. An illustration of a dual-hop short packet communication system.**

## II. SYSTEM MODEL

A cooperative SPC network is considered in Fig. 1, one source equipped with $N$ antennas, i.e., S, intends to transmit the information to its destination, i.e., D, with the assistance of one single antenna AF relay, i.e., R. It is assumed that the interference only affects on the relay due to the difference of frequency bands used in different two time-slots [12], [13], [23], [24], [25]. Frequency channel reuse can enhance the spectrum utilization in wireless systems, however, this also poses challenges for devices that share the same spectrum, as they may generate co-channel interference. In this paper, we assume that the relay experiences co-channel interference from $M$ other sources that use the same spectrum. Regarding applications, the proposed system can be deployed in a smart factory, where the source, i.e. the central controller,

**TABLE 1.** The important contributions of this paper compared to the existing works.

| Context | [14] | [5] | [6, 18, 20] | [7] | [12] | [13] | [15, 17] | [19, 21] | [22] | This work |
|---|---|---|---|---|---|---|---|---|---|---|
| Dual-hop | | ✓ | ✓ | ✓ | ✓ | ✓ | ✓ | ✓ | ✓ | ✓ |
| Multi-antennas | ✓ | | | | | | ✓ | | | ✓ |
| Co-channel interference | | | | | ✓ | ✓ | | | | ✓ |
| SPC | | | ✓ | | | | ✓ | ✓ | ✓ | ✓ |
| Optimization | ✓ | | | | | ✓ | | ✓ | ✓ | ✓ |

communicates with the destination, i.e. the actuator through the relay, i.e. robot. For other application, in some remote areas, a base station (the source) sends information to an user (the destination) with the help of another user who acts as a relay. All channels are assumed to experience quasi-static Rayleigh fading [12], [26], [27].

In this paper, owing to multiple antenna relays, we consider two transmission schemes, i.e., transmit antenna selection (TAS) scheme and beamforming scheme using maximum ratio transmission (BF-MRT) at the source. The signal transmission from S to D occurs in two time-slots (TSs).

### A. TAS SCHEME

In the first TS, S receives feedback from R to choose the index of the antenna having a maximum value of signal-to-noise ratio (SNR) [15] and this is mathematically expressed as

$$s = \arg \max_{1,\dots,N} |h_i|^2, \tag{1}$$

where $h_i$ is the channel of the link of the $i$-th antenna at S and R. Then, with the selected antenna, S transmits the signal, i.e., $x_s$, to the relay with the transmit power $P_{\mathrm{S}}$. Due to the presence of $M$ number of co-channel interferers, the received signal at R is expressed as

$$y_{\mathrm{R}}^{TAS} = \sqrt{P_{\mathrm{S}}} h_s x_s + \sum_{l=1}^{M} \sqrt{P_l} q_{l\mathrm{R}} x_l + n_{\mathrm{R}}, \tag{2}$$

where $P_l$, $x_l$ are the transmit power, the signal of the $l$-th interfere, respectively, and $q_{l\mathrm{R}}$ is channel coefficient for the $l$-th interfere-R link, $n_{\mathrm{R}} \sim \mathcal{CN}(0, \sigma_{\mathrm{R}}^2)$ presents the additive white Gaussian noise (AWGN) at the relay.

### B. BF-MRT SCHEME

In this scheme, S uses beamforming technique to transmit the signal to R. Hence, the received signal at R is expressed as

$$y_{\mathrm{R}}^{BF} = \sqrt{P_{\mathrm{S}}} \mathbf{h}^{\mathsf{T}} \mathbf{w}_s x_s + \sum_{l=1}^{M} \sqrt{P_l} q_{l\mathrm{R}} x_l + n_{\mathrm{R}}, \tag{3}$$

where $\mathbf{h}$ is $N \times 1$ channel vector of the S $-$ R link, $\mathbf{w}_s = \frac{|\langle|}{||\mathbf{h}||}$ denotes $N \times 1$ transmit weight vector and $(.)^{\mathsf{T}}$ is conjugate transpose.

Next, in the second TS, the signal $y_{\mathrm{R}}^{\lambda}$ with $\lambda \in \{TAS, BF\}$ is scaled with the amplification factor

$$G_v^{\lambda} = \sqrt{P_{\mathrm{R}} / \left( P_{\mathrm{S}} h^{\lambda} + \sum_{l=1}^{M} P_l |q_{l\mathrm{R}}|^2 + \sigma_{\mathrm{R}}^2 \right)}, \tag{4}$$

where $h^{TAS} = |h_s|^2$ for TAS, $h^{BF} = ||\mathbf{h}||^2$ and the relay forwards the version signal to D. Hence, the form of the signal at D is calculated as

$$y_{\mathrm{D}} = G_v^{\lambda} g y_{\mathrm{R}}^{\lambda} + n_{\mathrm{D}}, \tag{5}$$

where $g$ and $n_{\mathrm{D}} \sim \mathcal{CN}(0, \sigma_{\mathrm{D}}^2)$ are the channel coefficient between R and D, and the AWGN at D, respectively, $y_{\mathrm{R}}^{\lambda}$ is given in (2) for TAS scheme and (3) for BF-MRT scheme. Hence, we express the end-to-end (e2e) SINR of D as follow

$$\gamma_{\mathrm{D}}^{\lambda} = \frac{P_{\mathrm{S}} h^{\lambda} |g|^2}{|g|^2 (\sum_{l=1}^{M} P_l |q_{l\mathrm{R}}|^2 + \sigma_{\mathrm{R}}^2) + \sigma_{\mathrm{D}}^2 / (G_v^{\lambda})^2}, \tag{6}$$

where $G_v^{\lambda}$ is given in (4).

Substituting (4) into (6), the e2e SINR can be expressed as [12] and [13]

$$\gamma_{\mathrm{D}}^{\lambda} = \frac{X^{\lambda} Y}{V(Y+1) + X^{\lambda}}, \lambda \in \{TAS, BF\} \tag{7}$$

where $X^{\lambda} = P_{\mathrm{S}} h^{\lambda}$, $Y = \frac{P_{\mathrm{R}} |g|^2}{\sigma_{\mathrm{D}}^2}$ and $V = \sum_{l=1}^{M} P_l |q_{l\mathrm{R}}|^2$.

## III. PERFORMANCE ANALYSIS

Before calculating the BLER of the destination, we present the preliminaries that any SPC network should consider.

### A. PRELIMINARIES

For a given $\mathcal{N}$, i.e., the number of the information bit transmitted to D and $\mathcal{L}$, i.e., the block-length (packet length) or the number of channel use, the e2e average BLER for decoding the signal $x_s$ at D can be approximated by [28]

$$e_{\mathrm{D}}^{\lambda} = Q\left( \frac{C(\gamma_{\mathrm{D}}^{\lambda}) - r}{\sqrt{U(\gamma_{\mathrm{D}}^{\lambda})/\mathcal{L}}} \right), \lambda \in \{TAS, BF\}, \tag{8}$$

where $Q(q) = \int_q^{\infty} \frac{1}{\sqrt{2\pi}} e^{-y^2/2} dy$, $C(q) = \log_2(1+q)$ are the Gaussian Q-function, the Shannon capacity, respectively, and $U(q) = \log_2(e)^2 (1 - 1/(1+q))$ is the channel dispersion, $r \triangleq \mathcal{N}/\mathcal{L}$. Moreover, an approximation of $Q\left( \frac{C(\gamma_{\mathrm{D}}^{\lambda}) - r}{\sqrt{U(\gamma_{\mathrm{D}}^{\lambda})/\mathcal{L}}} \right)$

can expressed as [29, Appendix A].

$$\chi(\gamma_{\rm D}^{\lambda}) \approx \begin{cases} 1, & \gamma_{\rm D}^{\lambda} \le v, \\ 0, & \gamma_{\rm D}^{\lambda} \ge u, \\ \frac{1}{2} - \Xi(\gamma_{\rm D}^{\lambda} - \tau), & \text{otherwise}, \end{cases} \tag{9}$$

where $\Xi = [2\pi(2^{2r}-1)/\mathcal{L}]^{-1/2}$, $\tau = 2^r - 1$, $v = \tau - 1/(2\Xi)$, and $u = \tau + 1/(2\Xi)$. By suBFtituting (9) into (8), $e_{\rm D}^{\lambda}$ is attained as

$$e_{\rm D}^{\lambda} \approx \int_0^{\infty} \chi(\gamma_{\rm D}^{\lambda}) f_{\gamma_{\rm D}^{\lambda}}(x)dx \approx \Xi \int_v^u F_{\gamma_{\rm D}^{\lambda}}(x)dx. \tag{10}$$

### B. CDF DERIVATION

In this subsection, we derive cumulative distribution functions (CDFs) of $\gamma_{\rm D}^{TAS}$ for TAS scheme and $\gamma_{\rm D}^{BF}$ for BF-MRT scheme.

#### 1) TAS SCHEME

Since $X^{TAS} = P_{\rm S}h_s$ is Rayleigh distributed random variable, hence the CDF and probability density function (PDF) of the variable are

$$F_{X^{TAS}}(x) = 1 - \sum_{i=1}^{N} \binom{N}{i} (-1)^{i-1} \exp(-ix/\Psi_{\rm S}) \tag{11}$$

and

$$f_{X^{TAS}}(x) = \sum_{i=1}^{N} \binom{N}{i} (-1)^{(i-1)} (i/\Psi_{\rm S}) \exp(-ix/\Psi_{\rm S}), \tag{12}$$

respectively, where $\Psi_{\rm S} = P_{\rm S}\Omega_{\rm S}$, $\Omega_{\rm S} = (d_{\rm SR})^{-\theta}$ in which $d_{\rm SR}$ is the distance between S and R, $\theta$ is the path loss exponent. The PDF of $Y$ variable is

$$f_{\rm Y}(y) = \frac{1}{\Psi_{\rm D}} \exp\left(\frac{-y}{\Psi_{\rm D}}\right), \tag{13}$$

where $\Psi_{\rm D} = \frac{P_{\rm R}\Omega_{\rm D}}{\sigma_{\rm D}^2}$, $\Omega_{\rm D} - (d_{\rm RD})^{-\theta}$ in which $d_{\rm RD}$ is the distance between R and D.

Since $q_{l\rm R}$, $l = 1,\ldots, M$ are Rayleigh distributed random variables, hence the PDF of $V$ is [27, Eq. (7)]

$$f_V(v) = \frac{1}{\bar{\Psi}_{\rm IR}^M} \frac{v^{M-1}}{(M-1)!} \exp\left(\frac{-v}{\bar{\Psi}_{\rm IR}}\right), \tag{14}$$

where $\bar{\Psi}_{\rm IR} = \frac{P_l\bar{\Omega}_{\rm IR}}{\sigma_{\rm D}^2}$, $\bar{\Omega}_{\rm IR} = (\bar{d}_{\rm IR})^{-\theta}$ in which $\bar{d}_{\rm IR}$ is the average distance between the interferers and R.

*Proposition 1:* The CDF expression of $\gamma_{\rm D}^{TAS}$ given in (6), is obtained as

$$\begin{aligned} F_{\gamma_{\rm D}^{TAS}}(z) &= 1 - \sum_{i=1}^{N} \binom{N}{i} \frac{(-1)^{i-1}\exp(-z/\Psi_{\rm R})}{\bar{\Psi}_{\rm IR}(M-1)!} \\ &\times \Gamma(M+1)\Gamma(M) \exp\left(\frac{\beta^2}{2\alpha}\right) \alpha^{-M} W_{-M,\frac{1}{2}}\left(\frac{\beta^2}{\alpha}\right), \end{aligned} \tag{15}$$

where $\alpha = \left(iz/\Psi_{\rm S} + 1/\bar{\Psi}_{\rm IR}\right)$, $\beta = \sqrt{iz(z+1)/(\Psi_{\rm S}\Psi_{\rm R})}$, $W_{.,.}(.)$ is Whittaker function [30].

*Proof:* See Appendix A. ■

#### 2) BF-MRT SCHEME

Based on the CDF of variable $X^{BF} = P_{\rm S}||\mathbf{h}||^2$ being

$$F_{X^{BF}} = 1 - \exp\left(\frac{-x}{\Psi_{\rm S}}\right) \sum_{i=0}^{N-1} \frac{1}{i!} \left(\frac{x}{\Psi_{\rm S}}\right)^i, \tag{16}$$

the PDFs of $Y$ and $V$ given in (13) and (14), respectively, we obtain the CDF of $\gamma_{\rm D}^{BF}$ as the following **Proposition**.

*Proposition 2:* The CDF expression of $\gamma_{\rm D}^{BF}$ is

$$\begin{aligned} F_{\gamma_{\rm D}^{BF}}(z) = 1 &- \sum_{i=0}^{N-1} \sum_{j=0}^{j} \binom{i}{j} \frac{\exp\left(\frac{-z}{\bar{\Psi}_{\rm R}}\right) z^{(i+1)} \Psi_{\rm R}^{(j-i-1)/2}}{(\bar{\Psi}_{\rm IR})^M \Psi_{\rm S}^{(j+i+1)/2} i!(M-1)!} \\ &\times \Gamma(M+j+1)\Gamma(M+i) \frac{\exp\left(\frac{\bar{\beta}^2}{2\bar{\alpha}}\right) \bar{\alpha}^{L+(j+i)/2}}{\bar{\beta}} \\ &\times W_{-M-(i+j)/2,(j-i+1)/2}\left(\frac{\bar{\beta}^2}{\bar{\alpha}}\right), \end{aligned} \tag{17}$$

where $\bar{\alpha} = z/\Psi_{\rm S} + 1/\bar{\Psi}_{\rm IR}$, $\bar{\beta} = \sqrt{(z^2+z)/(\Psi_{\rm S}\Psi_{\rm R})}$.

*Proof:* See Appendix B. ■

### C. AVERAGE BLER

Due to the complexity of the CDF given in (15), it becomes difficult to calculate the integral presented in (10). To derive the expression for the average BLER while remaining high accuracy and low complexity, we apply an approach which is the first order Riemann integral approximation $\int_{t_1}^{t_2} f(x)dx = (t_2 - t_1) f(\frac{t_1+t_2}{2})dx$ used widely in the literature [31]. Hence, the average BLER of D is obtained as

$$e_{\rm D}^{\lambda} = (u-v) F_{\gamma_{\rm D}^{\lambda}}\left((u+v)/2\right), \lambda \in \{TAS, BF\}. \tag{18}$$

### D. ASYMPTOTIC ANALYSIS

When $P_{\rm S,R}$ go to infinity, the SINR of D reduces to

$$\gamma_{\rm D}^{\lambda,\infty} = \frac{X^{\lambda}Y}{VY + X^{\lambda}}, \lambda \in \{TAS, BF\}, \tag{19}$$

Then, we obtain CDF of $\gamma_{\rm D}^{\lambda,\infty}$ as the following **Proposition**.

*Proposition 3:* The CDF expressions of $\gamma_{\rm D}^{TAS,\infty}$ and $\gamma_{\rm D}^{BF,\infty}$ given in (19) are expressed as

$$\begin{aligned} F_{\gamma_{\rm D}^{TAS}}^{\infty}(z) = 1 &- \sum_{i=1}^{N} \frac{C_i^N (-1)^{i-1} \exp(-z/\Psi_{\rm R})}{\bar{\Psi}_{\rm IR}(M-1)!} \Gamma(M+1) \\ &\times \Gamma(M) \exp\left(\frac{\beta^2}{2\alpha}\right) \alpha^{-M} W_{-M,\frac{1}{2}}\left(\frac{(\beta_{asm}^{TAS})^2}{\alpha}\right), \end{aligned} \tag{20}$$

where $\beta_{asm}^{TAS} = \sqrt{iz^2/(\Psi_S\Psi_R)}$, $C_i^N = \binom{N}{i}$,

$$F_{\gamma_D^{BF}}^{\infty}(z) = 1 - \sum_{i=0}^{N-1}\sum_{j=0}^{j}\binom{i}{j}\frac{\exp\left(\frac{-z}{\Psi_R}\right) z^{(i+1)}\Psi_R^{(j-i-1)/2}}{(\bar{\Psi}_{IR})^M \Psi_S^{(j+i+1)/2} i!(M-1)!} \times \Gamma(M+j+1)\Gamma(M+i)\frac{\exp\left(\frac{\bar{\beta}^2}{2\bar{\alpha}}\right)\bar{\alpha}^{L+(j+i)/2}}{\beta_{asm}^{BF}} \times W_{-M-(i+j)/2,(j-i+1)/2}\left(\frac{(\beta_{asm}^{BF})^2}{\bar{\alpha}}\right), \quad (21)$$

where $\beta_{asm}^{BF} = \sqrt{z^2/(\Psi_S\Psi_R)}$.

Similarly, from **Proposition 2** and using the first order Riemann integral approximation, we get the approximated expression of the average BLER of D as

$$e_D^{\lambda,\infty} = (u-v)F_{\gamma_D^{\lambda}}^{\infty}((u+v)/2). \quad (22)$$

## IV. POWER CONTROL ISSUE

In this section, a solution of power allocation for maximizing the e2e effective throughput of the system is proposed. As defined in [32], the e2e effective throughput is expressed as

$$\tau^{\lambda} = r(1-e_D^{\lambda}), \lambda \in \{TAS, BF\}, \quad (23)$$

where $r = \mathcal{N}/\mathcal{L}$, $e_D^{\lambda}$ is given in (18). With the fixed location of the relay, we aim to optimize transmit power allocation to maximize the effective throughput:

$$(P_1): \max_{\{P_S,P_R\}} \tau^{\lambda}, \lambda \in \{TAS, BF\} \quad (24)$$

$$\text{s.t. } P_S + P_R \le P_t, \quad (24a)$$

$$P_S \ge 0,\ P_R \ge 0, \quad (24b)$$

where $P_t$ is the transmit power budget. Obviously, $\tau^{\lambda}$ is a decreasing function with $e_D^{\lambda}$, thus, Problem $P_1$ is equivalent as

$$(P_2): \min_{\{P_S,P_R\}} e_D^{\lambda}, \lambda \in \{TAS, BF\}$$

$$\text{s.t. } (24a), (24b). \quad (25)$$

However, it is difficult to determine the solution to Problem $P_2$ when substituting (18) into (25) since CDF in (15) is complicated. To overcome this issue, we provide the following **Lemma**.

*Lemma 1:* The BLER $e_D^{\lambda}$ is a decreasing function of $\gamma_D^{\lambda}$.

*Proof:* See Appendix C.

Based on *Lemma 1*, Problem $P_2$ can be transformed as

$$(P_3): \max_{\{P_S,P_R\}} \gamma_D^{\lambda}, \lambda \in \{TAS, BF\} \text{ s.t. } (24a), (24b). \quad (26)$$

Note that the first order derivatives of $\gamma_D^{\lambda}$ w.r.t $P_S$ and $P_R$ are positive,

i.e.,

$$\frac{\partial\gamma_D^{\lambda}}{\partial P_S} = \frac{VY(Y+1)h^{\lambda}}{(h^{\lambda}P_S + VY + V)^2} > 0,$$

$$\frac{\partial\gamma_D}{\partial P_R} = \frac{\frac{|g|^2}{\sigma^2}X(V+X^{\lambda})}{(V(\frac{|g|^2}{\sigma^2}P_R + 1) + X^{\lambda})^2} > 0,$$

where $X^{\lambda}$, $Y$ and $V$ are given in (6). Thus, $\gamma_D^{\lambda}$ are increasing functions of $P_S$ and $P_R$. Therefore, maximal $\gamma_D^{\lambda}$ requires maximized transmit power budget, i.e., $P_S + P_R = P_t$. Substituting $P_R = P_t - P_S$ into Problem $P_3$, it is easily known that $\gamma_D^{\lambda}$ is a concave function since the second order derivative of $\gamma_D^{\lambda}$ is negative, i.e.,

$$\frac{\partial^2\gamma_D^{\lambda}}{\partial P_S^2} = -\frac{2h^{\lambda}\frac{|g|^2}{\sigma^2}\left(\frac{|g|^2}{\sigma^2}P_tV + V\right)\left(h^{\lambda}P_t + V\right)}{\left(\frac{|g|^2}{\sigma^2}V(P_t - P_S) + h^{\lambda}P_S + V\right)^3} < 0. \quad (27)$$

Thus, by solving $\frac{\partial\gamma_D^{\lambda}}{\partial P_S} = 0$, the optimal value of $P_S^*$ can be obtained as

$$P_S^* = \begin{cases} \dfrac{\sqrt{\Delta_1\Delta_2} + \Delta_2}{V|g|^2/\sigma^2 - Vh^{\lambda}}, & V|g|^2/\sigma^2 - h^{\lambda} > 0, \\ \dfrac{-\sqrt{\Delta_1\Delta_2} + \Delta_2}{V|g|^2/\sigma^2 - Vh^{\lambda}}, & V|g|^2/\sigma^2 - h^{\lambda} < 0, \end{cases} \quad (28)$$

where $\Delta_1 = h^{\lambda}P_t + V$, $\Delta_2 = V|g|^2/\sigma^2P_t + V$. Finally, we have

$$P_R^* = P_t - P_S^*. \quad (29)$$

## V. NUMERICAL RESULTS

In this section, we provide simulations for validating the derived theoretical analysis. Unless otherwise stated, the parameters of the system are set in Table 2. For convenience, the transmit power of each interfer is set to be 2.8 dBm [12].

**TABLE 2. Parameter setting.**

| Parameter | Value |
|---|---|
| The number of bits, i.e., $\mathcal{N}$ | 100 (bits) [15] |
| $\theta$ | 3 |
| The number of packet length, i.e., $\mathcal{L}$ | 200 (channel uses) [33] |
| $\sigma_R^2 = \sigma_D^2 = \sigma^2$ | 1 |
| Distance between S and R, i.e., $d_{SR}$ | 30 (m) |
| Distance between R and D, i.e., $d_{RD}$ | 50 (m) |
| Distance between the $l$-th co-channel interference and R, i.e., $d_{lD}$ | random in 20 (m) to 50 (m) |

Fig. 2a and Fig. 2b illustrate that the BLERs of the destination change with respect to the total transmit power, i.e., $P_t$, for two schemes, i.e., optimal power allocation (opt.) and equal power allocation (eq.) with different the number of interferers in the TAS and BF-MRT methods, respectively. We set the number of antennas at S being 4. Obviously, when $P_t$ increases, the average BLERs significantly decrease. Under of impact of interference, the performance of the system degrades as the number of interferers increases. As expected, the performance of the optimal power allocation (OPA) scheme is always better than that of the equal power allocation (EPA) scheme. This verifies the proposed solution. Also, with large amount of co-channel interference, the performance of the OPA scheme is the same as the EPA scheme with small $P_t$, when $P_t$ is large enough, the OPA scheme is better than the EPA scheme. Furthermore, the simulation and theoretical curves match very well, which confirms that the mathematical derivations is correct.

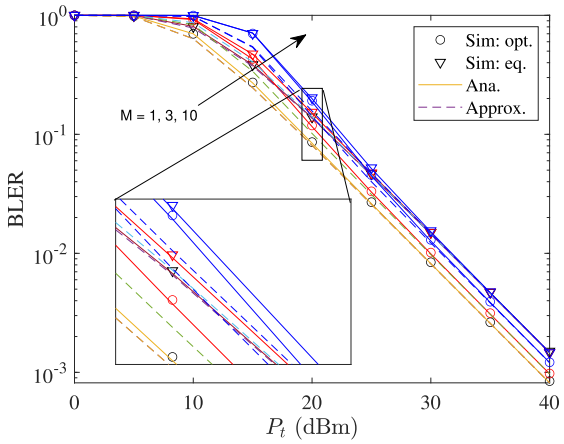


(a) TAS scheme

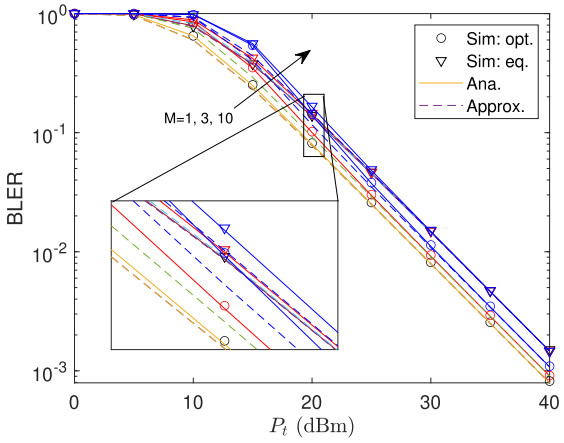


(b) BF-MRT scheme

**FIGURE 2.** Average BLERs versus $P_t$ for the optimal and equal power schemes, $N = 4$.

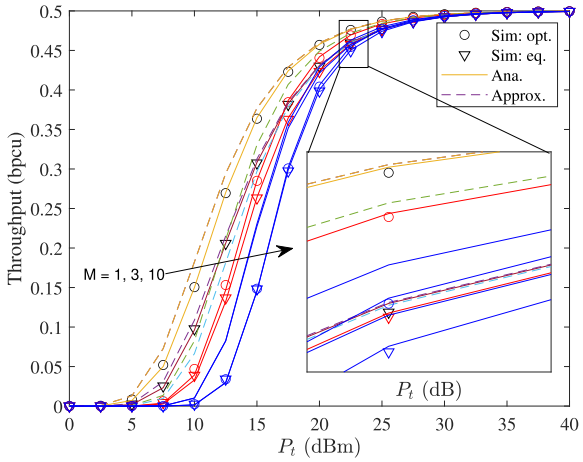


(a) TAS scheme

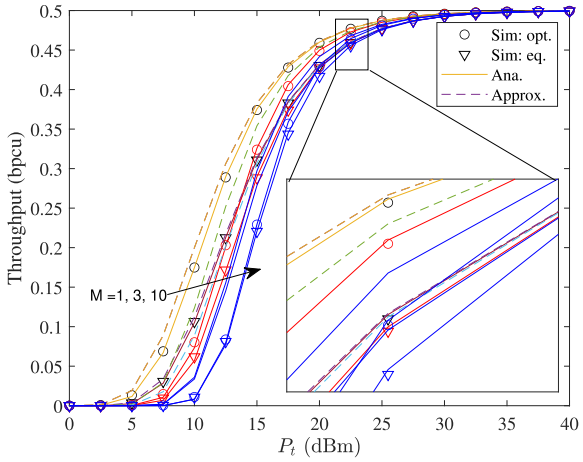


(b) BF-MRT scheme

**FIGURE 3.** Effective throughput versus $P_t$ for the optimal and equal power schemes, $N = 4$.

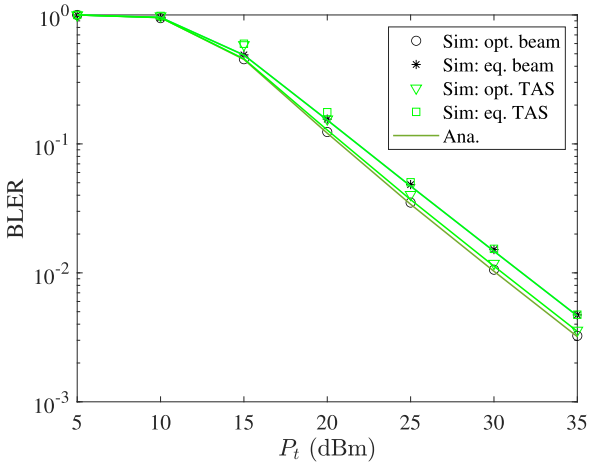


**FIGURE 4.** Average BLER versus $P_t$, $M = 8$ and $N = 4$.

Fig. 3a and Fig. 3b show the e2e throughput (bits per channel uses (bpcu)) versus $P_t$ with different the number of co-channel interference, i.e,. $M$ and the number of antennas at the source, i.e, $N$, being 4 for both the TAS and BF-MRT methods, respectively. Obviously, an increase in $P_t$ improves the system performance for both TAS and BF-MRT schemes. This is because increasing $P_t$ leads to better transmission quality or a decrease in BLER at the destination. In addition, when $P_t$ is sufficiently large, i.e., $P_t > 25$(dBm), the e2e throughput reaches saturation. It is clear that an increase in the number of co-channel interference sources results in degradation of the throughput. Once again, the performance of the OPA scheme confirms to be better than that of the EPA scheme.

For comparison, Fig. 4 plots the average BLER of the destination as a function of $P_t$ with $M = 8$ and $N = 4$. As $P_t$ increases, the BLER decreases significantly. At small $P_t$, i.e., $P_t < 15$ (dBm), the optimal algorithm does not show much advantage when the performance of optimal approaches is similar to equal power for both TAS and BF-MRT schemes. In addition, we can see that the performance of the BF-MRT scheme with the optimal transmit power (opt. beam) is better than that of TAS scheme with the optimal transmit power (opt. TAS) at large $P_t$. However, the performance gap

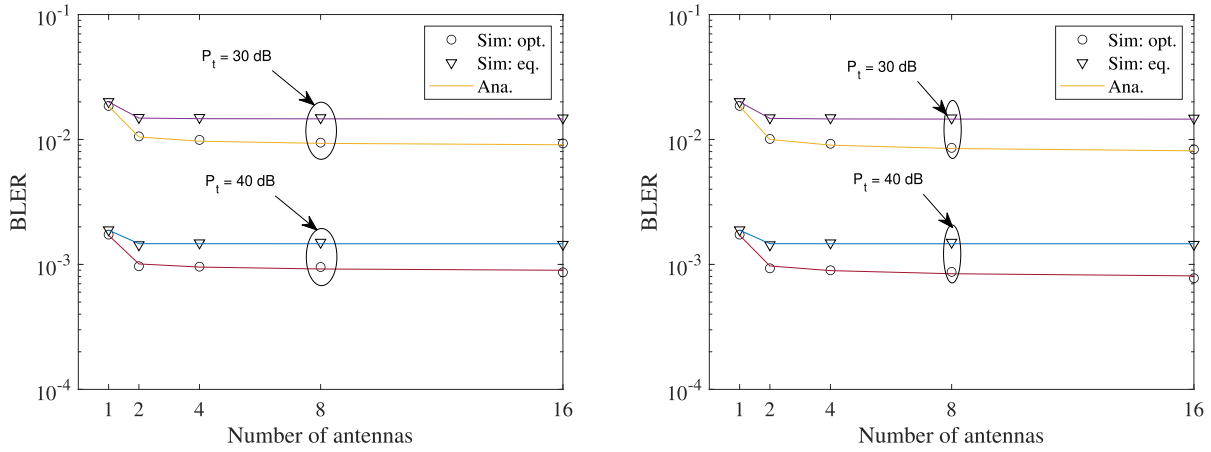


(a) TAS scheme (b) BF-MRT scheme

**FIGURE 5.** Average BLER versus number of antennas at the source, $M = 3$.

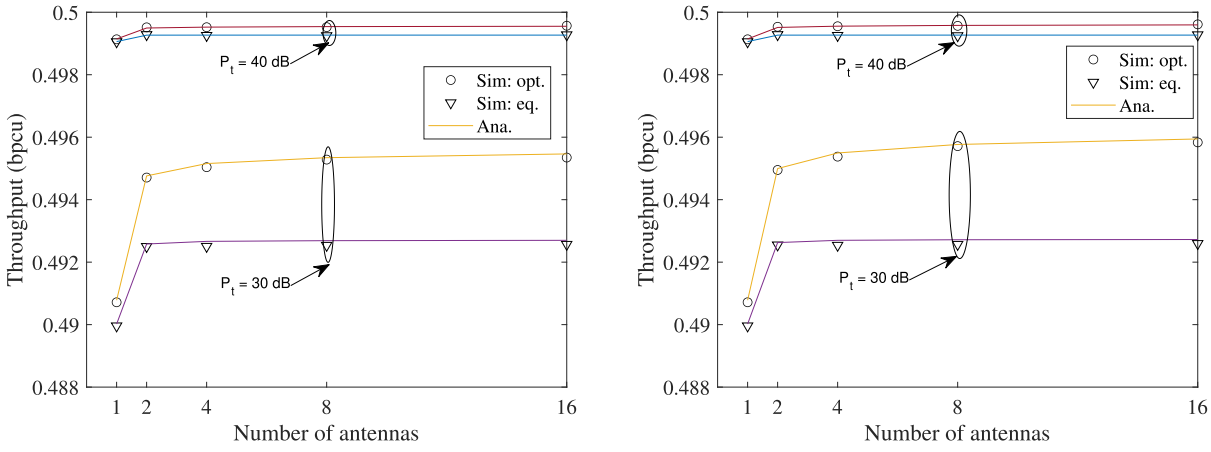


(a) TAS scheme (b) BF-MRT scheme

**FIGURE 6.** Effective throughput versus number of antennas at the source, $M = 3$.

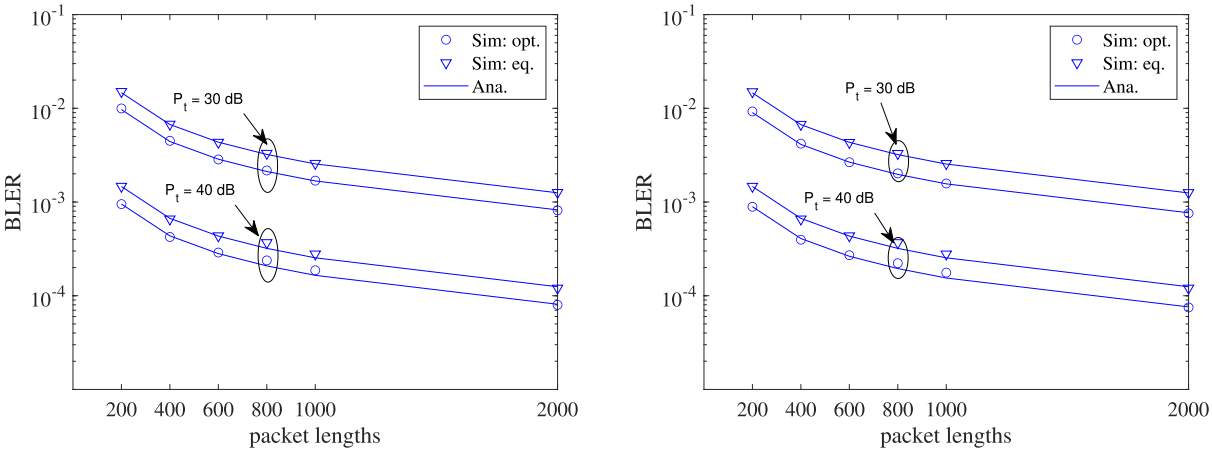


(a) TAS scheme (b) BF-MRT scheme

**FIGURE 7.** Average BLER versus the packet length.

is insignificant. For the equal power scheme (eq.), the average BLER of both the TAS and BF-MRT schemes are the same.

The impact of the number of antennas of the source are plotted in Fig. 5a and Fig. 5b for the TAS and

BF-MRT schemes, respectively, with different $P_t$ and $M = 3$. As can be seen that there is a decrease in the average e2e BLER as the number of antennas at S increases. This explains that more antennas at the source improves the transmission quality. However, the BLERs obtain saturation as increasing antennas at S. This is because the performance of the system depends on the weaker hop. As the number of antennas at S increases, the quality of the first hop improves but that of the second hop remains unchanged. As a result, the performance system depends on the second hop and reaches the saturation values.

The throughput affected by the deployment of antennas at the source are illustrated in Fig. 6a and Fig. 6b under different the total transmit power. With more antennas at S, the throughput is better and then reaches saturation value. The performance of the OPA-based system outperforms that of the EPA-based system for both TAS and BF-MRT schemes.

The BLERs evaluated with the change of packet lengths are shown in Fig. 7a and Fig. 7b with different $P_t$ for the TAS and BF-MRT schemes, respectively. Clearly, an increase in packet lengths results in the average e2e BLERs decrease. This means that the longer the packet length, the more accurately the signal is decoded. Additionally, the system's BLER decreases significantly when the packet length varies from 200 channel uses to 1000 channel uses. For packet lengths greater than 1000 channel uses, the reduction in BLER is negligible.

## VI. CONCLUSION

The paper presented short packet communications for relaying system under co-channel interference at the relay. Regarding deployment of multiple antenna at the source, we investigated two transmission methods, i.e., TAS and BF-MRT schemes. For performance evaluation, the closed-form and asymptotic expressions for BLERs of the system were derived for both TAS and BF-MRT schemes. In addition, we proposed an optimal power allocation for determining maximum the effective throughput of the system. The superiority of the proposed scheme was verified based on comparison of the equal power allocation scheme in terms of the BLERs and throughput. Also, the system performance was evaluated via important parameters such as the number of antennas deployed at the source, the packet-length, and the number of co-channel interference. In particular, the performance of the system improves as the number of antennas at the source increases, but it hits saturation with a high number of antennas. In order to overcome the drawback, deploying multiple antennas at the relay will be investigated in the future works. For extension, to service multiple destinations, non-orthogonal multiple access technique [29] should be applied in the system. In addition, presence of co-channel interference at both the relay and destination, as well as considering imperfect channel state information need to be evaluated in next papers.

## APPENDIX A
## PROOF OF PROPOSITION 1

From the given SINR in (6), the CDF of $\gamma_{\mathrm{D}}^{TAS}$ is calculated as

$$F_{\gamma_{\mathrm{D}}^{TAS}}(z) = \Pr\left[\frac{X^{TAS}Y}{X^{TAS} + V(Y+1)} < z\right]. \tag{30}$$

Eq. (30) is rewritten as

$$\begin{aligned}
F_{\gamma_{\mathrm{D}}^{TAS}}(z) &= 1 - \Pr\left[X^{TAS} > \frac{zV(Y+1)}{Y-z}, Y > z\right] \\
&= 1 - \int_z^\infty \int_0^\infty \left[1 - F_{X^{TAS}}\left(\frac{zv(y+1)}{y-z}\right)\right] \\
&\quad \times f_Y(y)dy f_V(v)dv \\
&\overset{(a)}{=} 1 - \left[\int_0^\infty \int_0^\infty \sum_{i=1}^{N} \binom{N}{i} (-1)^{(i-1)} \right. \\
&\quad \left. \times \frac{\exp\left(-\frac{z(w+z+1)v}{\Psi_{\mathrm{S}} w} - \frac{(w+z)}{\Psi_{\mathrm{R}}}\right)}{\Psi_{\mathrm{R}}} dw f_V(v)dv\right] \\
&\overset{(b)}{=} 1 - \int_0^\infty \sum_{i=1}^{N} \binom{N}{i} (-1)^{(i-1)} \frac{\exp\left(\frac{-z}{\Psi_{\mathrm{R}}}\right) 2\beta}{(\Psi_{IR})^M (M-1)!} \\
&\quad \times v^{M-1/2} \exp(-\alpha v) K_1(2\beta\sqrt{v}) dv,
\end{aligned} \tag{31}$$

where $f_Y(y)$, $f_V(v)$ are given in (13), (14), respectively, $\alpha = \left(\frac{iz}{\Psi_{\mathrm{S}}} + \frac{1}{\Psi_{IR}}\right)$, $\beta = \sqrt{\frac{iz(z+1)}{\Psi_{\mathrm{S}}\Psi_{\mathrm{R}}}}$, the step $(a)$ is to change variable $y$ to $w$, the step $(b)$ is attained with the help of [30, Eq. 3.324.1]. With the aid of [30, Eq. (6.643.3)], $F_{\gamma_{\mathrm{D}}^{TAS}}(z)$ is obtained as given in (15).

## APPENDIX B
## PROOF OF PROPOSITION 2

From the given SINR in (6), the CDF of $\gamma_{\mathrm{D}}^{BF}$ is calculated as

$$F_{\gamma_{\mathrm{D}}^{BF}}(z) = \Pr\left[\frac{X^{BF}Y}{X^{BF} + V(Y+1)} < z\right]. \tag{32}$$

Eq. (32) is rewritten as

$$\begin{aligned}
&F_{\gamma_{\mathrm{D}}^{BF}}(z) \\
&= 1 - \Pr\left[X^{BF} > \frac{zV(Y+1)}{Y-z}, Y > z\right] \\
&= 1 - \int_z^\infty \int_0^\infty \left[1 - F_{X^{BF}}\left(\frac{zv(y+1)}{y-z}\right)\right] f_Y(y)dy f_V(v)dv \\
&\overset{(w=y-z)}{=} 1 - \left[\int_0^\infty \int_0^\infty \sum_{i=0}^{N-1} \frac{\left(\frac{(z^2+wz+z)v}{w}\right)^i}{i!(\Psi_{\mathrm{S}})^i \Psi_{\mathrm{R}}} \right. \\
&\quad \left. \times \exp\left(-\frac{z(w+z+1)v}{\Psi_{\mathrm{S}} w} - \frac{(w+z)}{\Psi_{\mathrm{R}}}\right) dw f_V(v)dv.\right]
\end{aligned} \tag{33}$$

Let $\left(\frac{(z^2+wz+z)v}{w}\right)^i = \sum_{j=0}^{i} \binom{i}{j} z^i (z+1)^{(i-j)} w^{(j-i)}$ and after some mathematical arrangement, Eq. (33) can be rewritten

as

$$F_{\gamma_D^{BF}}(z) = 1 - \Bigg[ \int_0^\infty \sum_{i=0}^{N-1} \sum_{j=0}^{i} \binom{i}{j} \frac{\exp\left(\frac{-z}{\Psi_R} - \frac{zv}{\Psi_S}\right)}{i!(\Psi_S)^i \Psi_R} \times z^i (z+1)^{(i-j)} v^i \times \underbrace{\int_0^\infty w^{(j-i)} \exp\left(-\frac{z(z+1)v}{\Psi_S w} - \frac{w}{\Psi_R}\right) dw f_V(v) dv}_{I_v}. \Bigg] \tag{34}$$

With the aid of [30, Eq. (3.471.9)] for addressing $I_v$, suBFtituting (14) into Eq. 34 we have

$$F_{\gamma_D^{BF}}(z) = 1 - \sum_{i=0}^{N-1} \sum_{j=0}^{j} \binom{i}{j} \frac{\exp\left(\frac{-z}{\Psi_R}\right) z^{(i+1)} \Psi_R^{(j-i-1)/2}}{(\bar{\Psi}_{IR})^M \Psi_S^{(j+i+1)/2} i!(M-1)!} \times \int_0^\infty 2\, v^{(M+(j-i)/2-1/2)} \exp\left(-\left(\frac{z}{\Psi_S} + \frac{1}{\bar{\Psi}_{IR}}\right) v\right) \times K_{(j-i+1)}\left(2\sqrt{\frac{(z^2+z)v}{\Psi_S \Psi_R}}\right) dv. \Bigg] \tag{35}$$

With the aid of [30, Eq. (6.643.3)], we obtain the expression in (17).

## APPENDIX C
## PROOF OF LEMMA 1

For convenience, let denote $f(\gamma_D^\lambda) = \frac{C(\gamma_D^\lambda) - r}{\sqrt{V(\gamma_D^\lambda)/\mathcal{L}}}$, $\lambda \in \{TAS, BF\}$. Taking the first derivative of $e_D^\lambda$ w.r.t $\gamma_D^\lambda$, one have

$$\frac{\partial e_D^\lambda}{\partial \gamma_D^\lambda} = \frac{\partial e_D^\lambda}{\partial f(\gamma_D^\lambda)} \frac{\partial f(\gamma_D^\lambda)}{\partial \gamma_D^\lambda} - \frac{1}{\sqrt{(2\pi)}} e^{-(f^2(\gamma_D^\lambda)/2)} \times \underbrace{\frac{\sqrt{N}\left(1 - \frac{\ln 2(\log_2(1+\gamma_D^\lambda) - N/\mathcal{L})}{(1+\gamma_D^\lambda)^2 - 1}\right)}{\sqrt{(1+\gamma_D^\lambda)^2 - 1}}}_{W(\gamma_D^\lambda)}. \tag{36}$$

Note that $W(\gamma_D^\lambda) \geq \frac{\sqrt{N}\left(1 - \frac{\ln(1+\gamma_D^\lambda)}{(1+\gamma_D^\lambda)^2-1}\right)}{\sqrt{(1+\gamma_D^\lambda)^2-1}}$. We define $w(x) = \left(1 - \frac{\ln(x)}{x^2-1}\right)$ where $x = 1 + \gamma_D^\lambda \geq 1$. Considering the first derivative of $w(x)$ w.r.t $x$, we get

$$w'(x) = \frac{U(x)}{x(x+1)^2}, \tag{37}$$

where $U(x) = x^2 - 1 - 2x^2 \ln x$. Obviously, $U(x)$ is a decreasing function due to $U'(x) = -4x \ln(x) \leq 0$ for $x \geq 1$. Thus $U(x) \leq U(1) = 0$ holds, this results in $w'(x) \leq 0$ or $w(x)$ is a decreasing function of $x$ and $w(x) \leq w(1)$ for $x \geq 1$.

In addition, with $\lim_{x->1} w(x) = 1/2$ based on L'Hopital rule, we have

$$W(\gamma_D^\lambda) \geq \frac{\sqrt{N}}{2\sqrt{(1+\gamma_D^\lambda)^2 - 1}} \geq 0. \tag{38}$$

This leads to $(e_D^\lambda(\gamma_D))' \leq 0$.

## REFERENCES

[1] N. T. V. Khanh and T.-T. Nguyen, "Joint design of beamforming and antenna selection in short blocklength regime for URLLC in cognitive radio networks," *IEEE Access*, vol. 9, pp. 144676–144686, 2021.
[2] L. Liu and W. Yu, "A D2D-based protocol for ultra-reliable wireless communications for industrial automation," *IEEE Trans. Wireless Commun.*, vol. 17, no. 8, pp. 5045–5058, Aug. 2018.
[3] L. Yuan, N. Yang, F. Fang, and Z. Ding, "Performance analysis of UAV-assisted short-packet cooperative communications," *IEEE Trans. Veh. Technol.*, vol. 71, no. 4, pp. 4471–4476, Apr. 2022.
[4] T.-T. Nguyen, A.-V. Nguyen, T.-L. Nguyen, and V.-H. Le, "Two-way UAV-aided systems with short packet communications," *Comput. Netw.*, vol. 235, Nov. 2023, Art. no. 109957.
[5] P. Raut, P. K. Sharma, T. A. Tsiftsis, and Y. Zou, "Power-time splitting-based non-linear energy harvesting in FD short-packet communications," *IEEE Trans. Veh. Technol.*, vol. 69, no. 8, pp. 9146–9151, Aug. 2020.
[6] M. Fang, D. Li, H. Zhang, L. Fan, and I. Trigui, "Performance analysis of short-packet communications with incremental relaying," *Comput. Commun.*, vol. 177, pp. 51–56, Sep. 2021.
[7] T.-T. Nguyen and S. Q. Nguyen, "Short packet communications for cooperative UAV-NOMA-based IoT systems with SIC imperfections," *Comput. Commun.*, vol. 196, pp. 37–44, Dec. 2022.
[8] S. Q. Nguyen and H. Y. Kong, "Exact outage analysis of the effect of co-channel interference on secured multi-hop relaying networks," *Int. J. Electron.*, vol. 103, no. 11, pp. 1822–1838, Nov. 2016.
[9] S. Q. Nguyen and H. Y. Kong, "Outage probability analysis in dual-hop vehicular networks with the assistance of multiple access points and vehicle nodes," *Wireless Pers. Commun.*, vol. 87, no. 4, pp. 1175–1190, Apr. 2016.
[10] P. S. Lakshmi and M. G. Jibukumar, "A hybrid protocol for SWIPT in cooperative networks," *Adv. Electr. Electron. Eng.*, vol. 19, no. 1, Mar. 2021.
[11] D. Tung Vo, T. Van Chien, T. N. Nguyen, D.-H. Tran, M. Voznak, B. S. Kim, and L. T. Tu, "SWIPT-enabled cooperative wireless IoT networks with friendly jammer and eavesdropper: Outage and intercept probability analysis," *IEEE Access*, vol. 11, pp. 86165–86177, 2023.
[12] H. A. Suraweera, H. K. Garg, and A. Nallanathan, "Performance analysis of two hop amplify-and-forward systems with interference at the relay," *IEEE Commun. Lett.*, vol. 14, no. 8, pp. 692–694, Aug. 2010.
[13] F. S. Al-Qahtani, T. Q. Duong, C. Zhong, K. A. Qaraqe, and H. Alnuweiri, "Performance analysis of dual-hop AF systems with interference in Nakagami-*m* fading channels," *IEEE Signal Process. Lett.*, vol. 18, no. 8, pp. 454–457, Aug. 2011.
[14] N. H. Tu and K. Lee, "Performance analysis and optimization of multihop MIMO relay networks in short-packet communications," *IEEE Trans. Wireless Commun.*, vol. 21, no. 6, pp. 4549–4562, Jun. 2022.
[15] T.-T. Nguyen, T.-H. Vu, D. B. da Costa, P. X. Nguyen, and H. Q. Ta, "Short-packet communications in IoT-aided cellular cooperative networks with non-orthogonal multiple access," *IEEE Trans. Veh. Technol.*, vol. 72, no. 1, pp. 1296–1301, Jan. 2023.
[16] T.-V. Nguyen, V.-D. Nguyen, D. B. da Costa, T. Huynh-The, R. Q. Hu, and B. An, "Short-packet communications in multihop networks with WET: Performance analysis and deep learning-aided optimization," *IEEE Trans. Wireless Commun.*, vol. 22, no. 1, pp. 439–456, Jan. 2023.
[17] T.-H. Vu, T.-T. Nguyen, Q.-V. Pham, D. B. da Costa, and S. Kim, "A novel partial decode-and-amplify NOMA-inspired relaying protocol for uplink short-packet communications," *IEEE Wireless Commun. Lett.*, vol. 12, no. 7, pp. 1244–1248, Jul. 2023.
[18] L. Yuan, Q. Du, and F. Fang, "Performance analysis of full-duplex cooperative NOMA short-packet communications," *IEEE Trans. Veh. Technol.*, vol. 71, no. 12, pp. 13409–13414, Dec. 2022.

[19] J. Cheng and C. Shen, "Relay-assisted uplink transmission design of URLLC packets," *IEEE Internet Things J.*, vol. 9, no. 19, pp. 18839–18853, Oct. 2022.
[20] C. Guo, C. Guo, S. Zhang, and Z. Ding, "Adaptive relaying protocol design and analysis for short-packet cooperative NOMA," *IEEE Trans. Veh. Technol.*, vol. 72, no. 2, pp. 2689–2694, Feb. 2023.
[21] N. T. Y. Linh, N. H. Tu, P. N. Son, and V. N. Q. Bao, "Dual-hop relaying networks for short-packet URLLCs: Performance analysis and optimization," *J. Commun. Netw.*, vol. 24, no. 4, pp. 408–418, Aug. 2022.
[22] V. Shahiri, A. Kuhestani, and L. Hanzo, "Short-packet amplify-and-forward relaying for the Internet-of-Things in the face of imperfect channel estimation and hardware impairments," *IEEE Trans. Green Commun. Netw.*, vol. 6, no. 1, pp. 20–36, Mar. 2022.
[23] T. N. Nguyen, T. V. Chien, D.-H. Tran, V.-D. Phan, M. Voznak, S. Chatzinotas, Z. Ding, and H. V. Poor, "Security-reliability trade-offs for satellite-terrestrial relay networks with a friendly jammer and imperfect CSI," *IEEE Trans. Aerosp. Electron. Syst.*, vol. 59, no. 5, pp. 7004–7019, Oct. 2023.
[24] T. N. Nguyen, D.-H. Tran, T. Van Chien, V.-D. Phan, N.-T. Nguyen, M. Voznak, S. Chatzinotas, B. Ottersten, and H. V. Poor, "Physical layer security in AF-based cooperative SWIPT sensor networks," *IEEE Sensors J.*, vol. 23, no. 1, pp. 689–705, Jan. 2023.
[25] T. N. Nguyen, D.-H. Tran, T. Van Chien, V.-D. Phan, M. Voznak, and S. Chatzinotas, "Security and reliability analysis of satellite-terrestrial multirelay networks with imperfect CSI," *IEEE Syst. J.*, vol. 17, no. 2, pp. 2824–2835, Sep. 2022.
[26] T.-T. Nguyen, T.-V. Nguyen, T.-H. Vu, D. B. da Costa, and C. D. Ho, "IoT-based coordinated direct and relay transmission with non-orthogonal multiple access," *IEEE Wireless Commun. Lett.*, vol. 10, no. 3, pp. 503–507, Mar. 2021.
[27] S. S. Ikki, P. Ubaidulla, and S. Aissa, "Performance study and optimization of cooperative diversity networks with co-channel interference," *IEEE Trans. Wireless Commun.*, vol. 13, no. 1, pp. 14–23, Jan. 2014.
[28] Y. Polyanskiy, H. V. Poor, and S. Verdu, "Channel coding rate in the finite blocklength regime," *IEEE Trans. Inf. Theory*, vol. 56, no. 5, pp. 2307–2359, May 2010.
[29] T.-H. Vu, T.-V. Nguyen, T.-T. Nguyen, and S. Kim, "Performance analysis and deep learning design of wireless powered cognitive NOMA IoT short-packet communications with imperfect CSI and SIC," *IEEE Internet Things J.*, vol. 9, no. 13, pp. 10464–10479, Jul. 2022.
[30] A. Jeffrey and D. Zwillinger, *Table of Integrals, Series, and Products*. Amsterdam, The Netherlands: Elsevier, 2007.
[31] C. D. Ho, T.-V. Nguyen, T. Huynh-The, T.-T. Nguyen, D. B. da Costa, and B. An, "Short-packet communications in wireless-powered cognitive IoT networks: Performance analysis and deep learning evaluation," *IEEE Trans. Veh. Technol.*, vol. 70, no. 3, pp. 2894–2899, Mar. 2021.
[32] K. Wang, C. Pan, H. Ren, W. Xu, L. Zhang, and A. Nallanathan, "Packet error probability and effective throughput for ultra-reliable and low-latency UAV communications," *IEEE Trans. Commun.*, vol. 69, no. 1, pp. 73–84, Jan. 2021.
[33] T.-H. Vu, T.-V. Nguyen, D. B. da Costa, and S. Kim, "Intelligent reflecting surface-aided short-packet non-orthogonal multiple access systems," *IEEE Trans. Veh. Technol.*, vol. 71, no. 4, pp. 4500–4505, Apr. 2022.

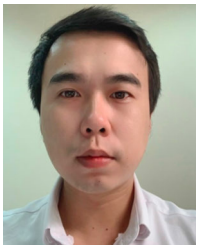

**QUANG-SANG NGUYEN** received the B.E. degree from Ho Chi Minh City University of Transport, Ho Chi Minh City, Vietnam, in 2010, the M.E. degree from Ho Chi Minh City University of Technology, Ho Chi Minh City, in 2013, and the Ph.D. degree in electrical engineering from the University of Ulsan, Ulsan, South Korea, in 2017. From January 2017 to June 2017, he was a Postdoctoral Research Fellow with Queen's University Belfast, Belfast, U.K. From June 2017 to May 2021, he was a Lecturer with Duy Tan University, Ho Chi Minh City. Since May 2021, he has been the Head of the Science of International Cooperation Department and a Lecturer with Ho Chi Minh City University of Transport. Since 2023, he has also been the Dean of the Faculty of Electrical and Electronic Engineering, Ho Chi Minh City University of Transport. His major research interests include cooperative communication, cognitive radio networks, physical layer security, energy harvesting, non-orthogonal multiple access, and artificial intelligence.

**UYEN-VU LE ANH** received the first B.Sc. degree from the University of Transport and Communications Campus in HCMC, Vietnam, in 1997, the dual M.Sc. degrees from Ho Chi Minh City University of Technology, Vietnam, in 2006 and 2008, respectively, and the second B.Sc. degree from the University of Transport and Communications Campus in HCMC, Vietnam, in 2022. Since 2003, she has been a Lecturer with the University of Transport and Communications. Her research interests include emerging topics of wireless communication for 5G and 6G, including energy harvesting, physical layer security, cognitive radio, non-orthogonal multiple access (NOMA), short-packet communications, and the Internet of Things (IoT).

**TAN N. NGUYEN** (Member, IEEE) was born in Nha Trang, Vietnam, in 1986. He received the B.S. degree in electronics from Ho Chi Minh University of Natural Sciences, in 2008, the M.S. degree in telecommunications engineering from Vietnam National University, in 2012, and the Ph.D. degree in communications technologies from the Faculty of Electrical Engineering and Computer Science, VSB—Technical University of Ostrava, Czech Republic, in 2019. He joined the Faculty of Electrical and Electronics Engineering, Ton Duc Thang University, Vietnam, in 2013, and since then, he has been lecturing. His major research interests include cooperative communications, cognitive radio, signal processing, satellite communication, UAV, and physical layer security. He was the Editor-in-Chief of *Advances in Electrical and Electronic Engineering* journal, in 2023.

**TIEN-TUNG NGUYEN** received the B.Sc. and M.Sc. degrees from the University of Science Ho Chi Minh City, Vietnam, in 2005 and 2010, respectively, and the Ph.D. degree in electronics from Myongji University, South Korea, in 2021. Since 2011, he has been a Lecturer with the Industrial University of Ho Chi Minh City. His research interests include wireless communication for 5G and 6G, including energy harvesting, physical layer security, cognitive radio, non-orthogonal multiple access (NOMA), short-packet communications, the Internet of Things (IoT), unmanned aerial vehicle (UAV), and applications of optimization and machine learning for wireless communications.

**MIROSLAV VOZNAK** (Senior Member, IEEE) received the Ph.D. degree in telecommunications from the Faculty of Electrical Engineering and Computer Science, VSB—Technical University of Ostrava, and the Habilitation degree, in 2009. In 2017, he was appointed as a Full Professor in electronics and communications technologies. He is a Principal Investigator in the research project QUANTUM5 funded by NATO, which focuses on the application of quantum cryptography in 5G campus networks. He participated in six projects funded by EU in programs managed directly by European Commission. He has authored and coauthored more than 100 articles in SCI/SCIE journals. His research interests include ICT, especially on the quality of service and experience, network security, wireless networks, and big data analytics. According to the Stanford University study released, in 2020, he is one of the World's Top 2% of Scientists in networking and telecommunications, and information and communications technologies. He has served as the General Chair for the 11th IFIP Wireless and Mobile Networking Conference, in 2018, and the 24th IEEE/ACM International Symposium on Distributed Simulation and Real-Time Applications, in 2020.